SIMULATION STUDY OF THE ELASTIC MECHANICAL PROPERTIES OF HMX

Thomas D. Sewell
Theoretical Division
Detonation Theory and Application Group
Los Alamos National Laboratory
Los Alamos, NM 87545

Dmitry Bedrov and Grant D. Smith
Department of Materials Science & Engineering and
Department of Chemical & Fuels Engineering, University of Utah
Salt Lake City 84112

Atomistic simulations were used to calculate isothermal elastic properties for β-, α-, and δ-octahydro-1,3,5,7-tetranitro-1,3,5,7-tetrazocine (HMX). The room-temperature isotherm for each polymorph was computed in the pressure interval $0 \leq p \leq 10.6$ GPa. These were used to extract the isothermal bulk modulus K_T and its pressure derivative $K_T' = dK_T/dp$ using two fitting forms employed previously in experimental studies of the β-HMX equation of state. Issues pertaining to sensitivity of the fitted parameters to details of the fitting form chosen and the weighting scheme used in the fits are discussed. The complete elastic tensor for each polymorph was calculated at room temperature and atmospheric pressure using the strain-strain fluctuation formula of Rahman and Parrinello, from which bulk and shear moduli were extracted. We report a preliminary prediction of a phase transition from α-HMX to a new polymorph, α'-HMX, for pressures between 0.2 and 0.5 GPa.

INTRODUCTION

Mesomechanics simulations, in which microstructure in a heterogeneous material is spatially resolved within a continuum hydrodynamic computational framework, are increasingly used to understand the physical response, *e.g.*, thermal localization (hot spots) of plastic-bonded high explosives (PBXs) under

various loading scenarios.[1,2] The goal of such studies is to identify and characterize the essential dissipative processes that must be captured in order to provide reliable, physically-based subgrid physics models for use in predictive, macroscale engineering codes[3]. The development and parameterization of mesomechanical models presents a significant challenge, given the expense and practical difficulties associated with measurements of explosive properties for the thermodynamic conditions of interest. For example, measurement of melt properties for many high explosives (HEs) is extremely difficult, if not impossible, due to the rapidity and violence of their chemical reactions above the melting transition. We argue, however, that judicious application of molecular simulation tools for the calculation of appropriate properties is a viable strategy for obtaining information required as input to mesoscale equations of state.

The high explosive octahydro-1,3,5,7-tetranitro-1,3,5,7-tetrazocine is the energetic material in a number of high performance explosive formulations.[4] HMX exhibits three pure crystal polymorphs at ambient pressure. These are denoted β-,[5,6] α-,[7] and δ-HMX,[8] where they are listed in terms of stability with increasing temperature. The elastic mechanical response of HMX is a key ingredient in the formulation of a complete HMX equation of state. Two general experimental approaches have been applied to obtain the elastic properties of HMX: measurements of the isotherm, $V=V(p)$,[9,10], and determinations of isentropic sound speeds from impulsive stimulated light scattering methods (ISLS).[11] The isotherm can be used to obtain the isothermal bulk modulus K_T and its pressure derivative $K_T'=dK_T/dp$ *via* an assumed equation of state fitting form. ISLS sound speed measurements provide direct information about the isentropic elastic tensor, from which the bulk and shear moduli, as well as other engineering parameters can be extracted.

There are two published measurements of the room temperature isotherm for β-HMX. Olinger, Roof, and Cady reported an x-ray determination of the room temperature lattice parameters of β-HMX in the pressure interval $0 < p < 7.47$ GPa.[9] They fit the isotherm to an equation of state

$$p(V) = \frac{V_0 - V}{\left[V_0 - s_T\left(V_0 - V\right)\right]^2} c_T^2 \qquad (1)$$

based on the hugoniot jump conditions, [12]

$$\frac{V}{V_0} = 1 - \frac{U_p}{U_s}, \qquad (2)$$

$$p = p_0 + \rho_0 U_p U_s,$$

where V is specific volume; U_s and U_p are the pseudo shock velocity and pseudo particle velocities, respectively; ρ is density; and "0" denotes the reference state (atmospheric pressure in the present case). The fitting parameters c_T and s_T are related to the bulk modulus K_T and its pressure derivative K_T' as $K_T=\rho_0 c_T^2$ and $K_T'=4s_T-1$, respectively. In their analysis, Olinger *et al.* observed a linear relation between U_s and U_p, $U_s=c_T+s_T U_p$, and obtained K_T=13.5 GPa and K_T'=9.3.

More recently, Yoo and Cynn revisited the β-HMX isotherm.[10] Their synchotron x-ray determination of the pressure dependent lattice parameters extended the isotherm to 43 GPa (discovering two previously unreported phase transitions; including an apparent martensitic

transition at ~12 GPa, identified based on abrupt changes in the Raman spectrum; and second one with a 4% volume change at ~27 GPa.). They analyzed their data using the third-order Birch-Murnaghan equation of state[13]

$$p(V)=\tfrac{3}{2}K\left[\eta^{-7/3}-\eta^{-5/3}\right]\left[1+\tfrac{3}{4}\left(K'-4\right)\left(\eta^{-2/3}-1\right)\right] \quad (3)$$

where $\eta=V/V_0$ is the compression ratio at pressure p. Yoo and Cynn reported K_T=12.4 GPa and K_T'=10.4, for pressures below 27 GPa.

Menikoff and Sewell[14] recently reported a re-analysis of the experiments, applying both fitting forms to both data sets, in an attempt to reconcile the discrepancy between them and to determine which data set and fitting form combination is most consistent with the preponderance of other data for HMX and HMX-based PBXs. In the case of the Yoo-Cynn data, they also considered the sensitivity in the predicted values of K_T and K_T' to the interval of the data used, due to the presence of phase transitions. Although Menikoff and Sewell obtained values of K_T and K_T' that disagreed significantly with those reported by Yoo and Cynn, they found that their data, fit using the third-order Birch-Murnaghan equation of state, leads to better overall agreement with the other HMX data than does the Olinger-Roof-Cady set. On the basis of this study, Menikoff and Sewell concluded that the best one can say about K_T and K_T' at the time of their report is that K_T=14.3± 3.5 GPa and K_T'=7.5± 1.9. This is a large uncertainty in a parameter that figures prominently in the Mie-Gruneisen equation of state commonly used in mesoscale and engineering models of HMX.

Published information about the elastic tensor for β-HMX is limited to a partial determination, due to Zaug, at two temperatures.[11] By fitting to sound speeds determined from ISLS measurements, Zaug was able to obtain a set of elastic coefficients. With only two experimental samples of similar orientations available, however, the number of elastic coefficients projecting strongly onto the observed sound speeds was limited; indeed, only five of the thirteen non-zero elastic constants could be accurately determined (C_{11}, C_{15}, C_{33}, C_{35} and C_{55}). To determine a complete set of elastic coefficients corresponding to a globally optimized fit would require additional measurements for different crystal orientations.

The thermophysical and mechanical properties of HMX have been the subject of a number of atomistic simulation studies.[15-24] Sewell[16] used a rigid molecule force field, in conjunction with isothermal-isobaric Monte Carlo methods, to compute equilibrium structural parameters and the room temperature isotherm of β-HMX and RDX. He obtained good agreement with the data of Olinger *et al.*[9] for both materials. Thompson and co-workers have developed a "transferable" intermolecular force field,[25] and applied it to a number of high explosives. They calculated the isotherm for β-HMX,[18] and used the Murnaghan equation,

$$p(V)=\frac{K_T}{K_T'}\left[\left(\frac{V_0}{V}\right)^{K'}-1\right], \quad (4)$$

to obtain a values (K_T=14.53 GPa, K_T'=9.57) or (K_T=16.86 GPa, K_T'=9.50) for the bulk modulus and pressure derivative, using $P_{21/c}$ and $P_{21/n}$ space group settings, respectively. (This discrepancy is a point of some confusion, since the two space groups are

equivalent; one possible explanation is differences in molecular geometry associated with the two experimental structure determinations.)

Lewis and co-workers[19] reported quantum chemistry-based predictions of crystal structures for all three HMX polymorphs. They obtained a value of 12.5 GPa for the bulk modulus of β-HMX, based on a full optimization of the primary simulation cell contents and the three lattice lengths. (The lattice angles were constrained to experimental values.) Estimates for the bulk modulus of α- and δ-HMX were significantly larger, 38.6 and 48.0 GPa, respectively, but are highly suspect due to geometric constraints imposed during the optimizations, which almost certainly led to large non-hydrostatic elements in the stress tensor. (This fact was recognized and pointed out by the authors of that study.)

Bedrov *et al.* have reported previously calculations of the structural and elastic properties of the three pure crystal polymorphs,[22,23,24] and the temperature dependent shear viscosity[20] and thermal conductivity[21] of the liquid phase. The calculations were performed using atomistic molecular dynamics methods with a fully flexible, quantum chemistry-based force field.[26] Good agreement with experiment was obtained for equilibrium lattice parameters, linear and volumetric coefficients of thermal expansion, and heats of sublimation, ΔH_s, for each polymorph.[22,23] The predicted melt thermal conductivity is consistent with data for the solid state at elevated temperatures.[21]

The focus of the present work is the elastic mechanical properties of HMX polymorphs at room temperature and pressure. In particular, we calculate the room-temperature isotherm for each polymorph and extract the bulk modulus $K_T=-Vdp/dT$ and its pressure derivative $K_T'=dK/dp$ using the two fitting forms identified above. In the case of β-HMX, we compare our results to experiment. We apply formalism due to Rahman and Parrinello[27] to compute directly the second-order elastic tensor at room temperature and pressure. Beyond the fact that these properties are key elements in the description of the elastic mechanical response of HMX, additional points of interest are: (1) the level of internal consistency between values of the bulk modulus calculated directly from the elastic tensor to values obtained from the equation of state fitting forms, (2) the sensitivity of the latter to the form chosen and the details of how the fit is performed, and (3) the agreement between predicted results and the available experimental data. This article supercedes an initial report in an earlier conference proceeding.[24]

COMPUTATIONAL DETAILS

Calculations were performed in the isothermal-isobaric (*NpT*) statistical ensemble.[28] Periodic boundary conditions corresponding to a general, triclinic primary cell were used. The simulations were performed using the same force field as in our previous studies of HMX.[20-24] The development[26] and implementation[20,22] of the force field are described elsewhere. We note that our simulations include all degrees of freedom other than covalent bond stretching motions, which were constrained to equilibrium values using the SHAKE[28] algorithm. The effects of this constraint are expected to be small.

The β-, α-, and δ- phases of HMX are monoclinic[5,6] ($P_{21/c}$ or, equivalently, $P_{21/n}$ space group, Z=2 molecules per unit cell, symmetry axis = *b*; 13 independent elastic coefficients[29]), orthorhombic[7] (F*dd*2, Z=8; 9 independent elastic coefficients), and hexagonal[8] ($P6_1$, Z = 6, symmetry axis = *c*; 5 independent elastic coefficients), respectively. Primary simulation cells containing 96 molecules were used for β-HMX and δ-HMX, corresponding to 48 (4x3x4) and 16 (4x4x1) unit cells, respectively. Primary cells containing 64 molecules were used for α-HMX, corresponding to 8 (2x1x4) unit cells. Electrostatic interactions were treated using the standard Ewald summation.[28] Non-bonded interactions were truncated at 9 Å, 10 Å, and 10 Å for β-, α-, and δ-HMX, respectively. A fixed time step size of one fs was used in all cases. Equilibration runs of one ns duration were performed, followed by production runs of ten ns and two ns for p=1 atm and p > 1 atm, respectively, during which data were collected for subsequent analysis. All of the calculations were performed at 295 K.

We used *NVT-MD* to sample the contents of the simulation cell, and an *NpT-MC* Monte Carlo algorithm to vary its shape and volume. The latter moves were carried out as described previously,[16] within a rigid-molecule framework using the atomic positions at the end of the preceding *NVT-MD* sequence. In practice, 1000 fs of *NVT-MD* was followed by a sequence of 100 *NpT-MC* states. Thus, over the course of one ns accumulated *NVT* simulation time, 100,000 Monte Carlo states were sampled. The Monte Carlo step size for a given thermodynamic state was adjusted to yield an acceptance probability of 40-50%.

DATA ANALYSIS

We observed clear deviations from linearity at low pressures in our isotherms in the U_s-U_p plane, with increased compressibility of the crystal at pressures below one GPa. While such behavior would be anomalous for metals, it is actually expected in the case of polyatomic molecular crystals, due to complicated molecular packings and intramolecular flexibility, and has in fact been reported for the high explosive pentaerythritol tetranitrate (PETN).[30] We accommodated this nonlinearity in the U_s-U_p plane by fitting our results to quadratic form,

$$U_s = c_T + s_T U_p + q U_p^2 . \qquad (5)$$

We note that the third-order Birch-Murnaghan equation of state can be written as a linear function in K_T and $K_T K_T'$ *via* the transformation

$$x=[\eta^{-2/3}-1]^{-1}-3 \qquad (6)$$
$$y=2p(V)\{3[\eta^{-7/3}-\eta^{-5/3}][\eta^{-2/3}-1]\}^{-1},$$

for which the slope and intercept are K_T and $3K_T K_T'/4$, respectively. In this plane, low-pressure data points are more heavily weighted than high pressure ones. We argue that fits to obtain the initial bulk modulus and pressure derivative using the third-order Birch-Murnaghan equation of state should employ Eq. 6 rather than a direct fit of Eq. 3 in the *p*-*V* plane, for which all data points are weighted equally, regardless of pressure.

We have applied both the quadratic U_s-U_p and the two third-order Birch-Murnaghan fitting forms to the calculated isotherms. The results are compared to the experimental data, where available,

and to bulk modulus values obtained directly from the elastic tensor.

Rahman and Parrinello[27] showed that the fourth-rank elastic tensor for an anisotropic crystalline solid can be calculated using fluctuations of the microscopic strain tensor:

$$C_{ijkl} = \frac{\kappa T}{\langle V \rangle} \langle \varepsilon_{ij} \varepsilon_{kl} \rangle^{-1}, \qquad (7)$$

where $\langle V \rangle$ is the average volume at a given temperature T (and, implicitly, pressure p). The instantaneous strain tensor is given by

$$\varepsilon = \frac{1}{2}\left[\mathrm{h}_0^{-\mathrm{T}}\left(\mathrm{h}^{\mathrm{T}}\mathrm{h}\right)\mathrm{h}_0^{-1} - 1\right], \qquad (8)$$

where **h** is the matrix that transforms between cartesian and scaled coordinates, superscript "T" denotes matrix transpose, and $\mathbf{h}_0$ is the reference state of the system at a given p-T state, corresponding to the average volume and shape. Equations 7 and 8 are readily constructed from a suitably large set of observations from an isothermal-isobaric simulation. The fourth-rank elastic tensor **C** can be expressed as a 6x6 matrix using Voigt notation; details can be found elsewhere.[31] The particular form expected for **C** is determined by the symmetry class for a given crystal (*e.g.*, monoclinic, orthorhombic, and hexagonal for β-, α- and δ-HMX, respectively), and can be used as a partial check for convergence of the simulation results.

RESULTS AND DISCUSSION

Calculated and measured lattice parameters and unit cell volumes at 295 K and one atmosphere were compared for each HMX polymorph. We note that experimental determinations for all three cases were made under these conditions. The results are in good agreement with experiment. The average magnitude percent error in molecular volumes is 0.8%, with a maximum of 1.8% occurring for α-HMX. The average magnitude percent error in lattice lengths is 2.8%, 1.2%, and 1.8% for β-, α-, and δ-HMX, respectively; the maximum among all lattice lengths is 4.6%, for lattice length *b* in β-HMX.

Simulated and measured compression curves for β-HMX are shown in Fig. 2. The agreement between experiment and simulation is reasonably good: at the highest pressure considered here, 10.6 GPa, the percent difference between our compression ratio V/V_0 and that of Yoo and Cynn is 4.6%. The solid line passing through the simulation results is a fit of the third-order Birch-Murnaghan equation of state to the data using Eq. 6. Application of Eq. 5 to the β-HMX isotherm leads to the *Us*-*Up* curve shown

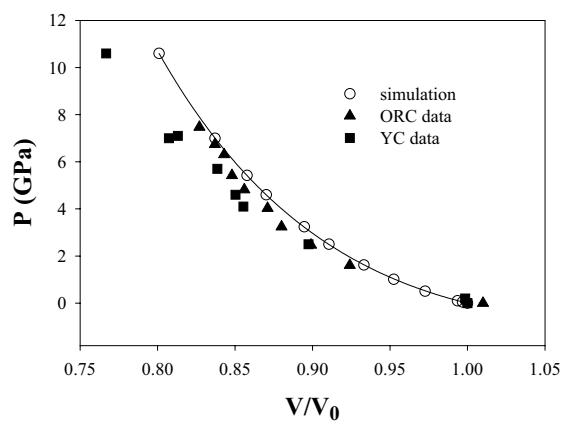

FIGURE. 1: ISOTHERMS FOR β-HMX AT 295 K. SIMULATION: THIS WORK; ORC: REF. 9; YC: REF. 10.

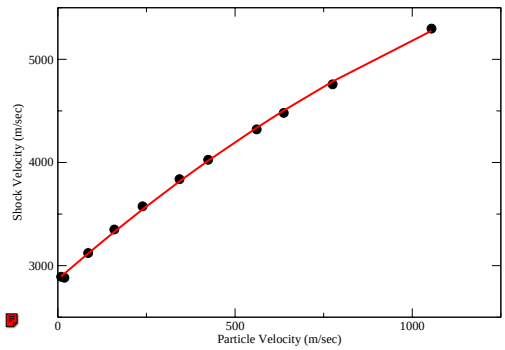

FIGURE 2. CALCULATED β-HMX ISOTHERM IN *Us-Up* PLANE. SOLID CURVE IS QUADRATIC FIT TO RESULTS.

in Fig. 2. Curvature of the results in this plane is clearly evident. Experimental studies of the isotherm typically provide little if any information for pressures below about one GPa, and thus estimates of sound speeds based on extrapolation of such data are likely to yield overestimates to true values.

The calculated elastic tensor for β-HMX is provided in Table 1, where values reported by Zaug[11] are also included. As mentioned above, Zaug's experiments sufficed to determine uniquely five of the thirteen elastic constants (*modulo* the need to specify a target value for the bulk modulus). These coefficients -- C_{11}, C_{33}, C_{55}, C_{15}, and C_{35} -- are shown in boldface in Table 1. The comparison between the two sets is most meaningful for those particular C_{ij}.

In Fig. 3 we summarize all of the data for the room temperature bulk modulus of β-HMX. Individual values of the bulk modulus in Fig. 3 are plotted along the ordinate, while the abscissa corresponds to source of information: the present simulation (simul), the data of Olinger,

TABLE 1. ELASTIC TENSOR FOR β-HMX AT 1 atm AND 295K.[a]

	β-HMX (expt)[b]	*β*-HMX (calc)
C_{11}	**20.8**	22.2±0.3
C_{22}	26.9	23.9±0.5
C_{33}	**18.5**	23.4±0.5
C_{44}	4.2	9.2±0.2
C_{55}	**6.1**	11.1±0.1
C_{66}	2.5	10.1±0.1
C_{12}	4.8	9.6±0.7
C_{13}	12.5	13.2±0.3
C_{23}	5.8	13.0±0.2
C_{15}	**-0.5**	-0.1±0.3
C_{25}	-1.9	4.7±0.2
C_{35}	**1.9**	1.6±0.2
C_{46}	2.9	2.5±0.3

[a]For *β*-HMX, *a* is directed along $\hat{\mathbf{x}}$, *b* is along $\hat{\mathbf{y}}$, and *c* is in the $\hat{\mathbf{x}}\hat{\mathbf{z}}$ plane, in a right-handed cartesian frame. Error bars reflect elastic coefficients computed from five sub-averages from the overall set of configurations. [b]Zaug[11] chose a different orientation in his experiments on *β*-HMX; we have transformed the elastic tensor presented in Ref. 11 to coincide with the choice made in the present work.

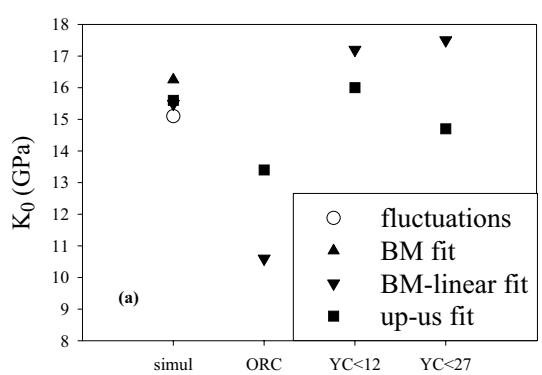

FIGURE 3: SUMMARY OF BULK MODULUS DATA FOR β-HMX.

Roof, and Cady (ORC), and Yoo & Cynn for limiting pressures of 12 GPa (YC<12) and 27 GPa (YC<27). Several points are to be noted. First, the bulk modulus derived from the calculated elastic tensor is equal within error bars to that obtained from an analysis of volume fluctuations, and are close to values obtained from EOS fits to the isotherm. The simulation predictions are in good agreement with results based on the Yoo and Cynn isotherm; the isotherm of Olinger *et al.* leads to a somewhat lower range of values. Menikoff and Sewell concluded that, between the two experimental isotherms, Yoo and Cynn's data are more consistent overall with other data for HMX and HMX-based explosives. However, values for *K* from their data and from the present simulations are larger by 2-3 GPa than is typically used in the Mie-Gruneisen equation of state commonly used for HMX.

Calculated isotherms for α- and δ-HMX are presented in Fig. 4. There are no experimental data available for comparison. The results for δ-HMX indicate a higher compressibility relative to β-HMX. For the case of α-HMX, the

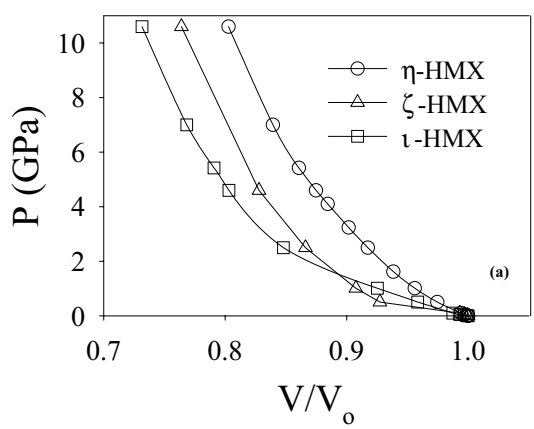

FIGURE 4. ISOTHERMS FOR HMX POLYMORPHS.

initial slope is comparable, but a clear break in the compression curve is observed between 2 and 5 kbar. This is discussed further below.

There are no previous reports concerning the elastic coefficients for *α*– and *δ*-HMX. The present results indicate considerable anisotropy in the principal elements of the tensor for *α*-HMX.

TABLE 2. ELASTIC TENSORS FOR α- AND δ-HMX AT 1 atm AND 295 K.[a]

	α-HMX	*δ*-HMX[b]
C_{11}	30.6±0.5	14.5±0.7
		$C_{11}=C_{22}$
C_{22}	23.3±0.8	14.0±0.8
		$C_{22}=C_{11}$
C_{33}	31.4±0.2	18.0±0.9
C_{44}	0.80±0.04	4.4±0.2
		$C_{44}=C_{55}$
C_{55}	3.3±0.1	4.4±0.2
		$C_{55}=C_{44}$
C_{66}	3.3±0.2	2.3±0.4
		C_{11}-C_{12}
C_{12}	5.7±0.7	10.3±0.5
C_{13}	13.8±0.7	10.6±0.7
		$C_{13}=C_{23}$
C_{23}	6.0±0.3	10.3±0.4
		$C_{23}=C_{13}$

[a]For *α*-HMX, *a*, *b*, and *c* are directed along the $\hat{\mathbf{x}}, \hat{\mathbf{y}}$, and $\hat{\mathbf{z}}$ axes, respectively, in a right-handed cartesian frame. For *δ*-HMX, *a* is directed along $\hat{\mathbf{x}}$, *b* is in the $\hat{\mathbf{x}}\hat{\mathbf{y}}$ plane, and *c* is along the $\hat{\mathbf{z}}$ axis
[b]Actual calculated values. Where shown, relations among the elastic constants reflect formal expectations based on crystal symmetry.

Formal, symmetry-based expectations for δ-HMX are satisfied to within estimated error, with the exception of C_{66}, for which the predicted value C_{66} = 2.3 GPa differs from the expected value $C_{66}=C_{11}-C_{13}$=3.9 GPa.

Bulk and shear moduli for all three HMX polymorphs are summarized in Table 3. Relative to β-HMX, the predicted bulk moduli of α- and δ-HMX differ by roughly 7% and 22%, respectively, and correlate reasonably well with crystal density. We note that the shear moduli of α- and δ-HMX are predicted to be, at most, half the value for β-HMX.

TABLE 3. BULK AND SHEAR MODULI FOR HMX AT 1 atm AND 295 K.

	β-HMX (expt)	*β*-HMX (calc)
K (GPa)	14.0±3.5[a]	15.1[b] 15.1, 15.7[c] 15.5[d]
G (GPa)		7.0, 8.3[c]
	α-HMX (calc)	*δ*-HMX (calc)
K (GPa)	14.1[b] 14.3, 15.1[c] 14.0[d]	11.8[b] 11.9, 12.1[c] 12.0[d]
G (GPa)	2.4, 5.5[c]	2.9, 3.2[c]

[a]Ref 14. [b]From volume fluctuations, using $K = \kappa T\langle V\rangle / \sigma_V^2$, where σ_V^2 is the Gaussian variance of the volume distribution from the simulation. [c]From the elastic tensor (Reuss average, Voigt average). [d]Third-order Birch-Murnaghan equation of state, fit using Eq. 6.

In light of the apparent break in the compression curve for α-HMX, we examined more closely the structures for simulations at two and five kbar. Snapshots for those two cases are shown in Fig. 5. A clear phase transition, involving both the molecular orientation and crystal symmetry class, but not the molecular point group, is observed. We emphasize that this is a preliminary result.

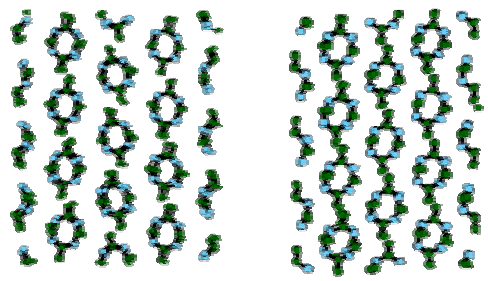

FIGURE 5. PRESSURE INDUCED PHASE TRANSITION IN α-HMX. VIEWS SHOW PROJECTION OF SIMULATION CELL BELOW (LEFT) AND ABOVE RIGHT) TRANSITION.

REFERENCES

[1] M.R. Baer, Thermochim. Acta **38**, 351 (2002).

[2] S.G. Bardenhagen, J.U. Brackbill, and D. Sulsky, Phys. Rev. E **62**, 3882 (2000).

[3] R. Menikoff and T.D. Sewell, Combust. Theor. Model. **6**, 103 (2002).

[4] Gibbs, T.R.; Popolato, A. *LASL Explosive Property Data* (University of California, Berkeley, 1980).

[5] C.S Choi and H.P. Boutin, Acta Crystallogr. B **26**, 1235 (1970).

[6] Kohno, Y.; Maekawa, K.; Azuma, N.; Tsuchioka, T.; Hashizume, T.; Imamura, A. *Kogyo Kayako* **53**, 227 (1992).

[7] Cady, H.H.; Larson, A.C.; Cromer, D.T. *Acta Cryst.* **16**, 617 **(1963)**. Note that the "*y*" fractional coordinate for atom N_1 in Table 2 should have a negative sign.
[8] Cobbledick, R.E.; Small, R. W. H. *Acta Cryst. B* **30**, 1918 (1974).
[9] B. Olinger, B. Roof, and H. Cady, "The linear and volume compression of β-HMX and RDX", in: Proc. Symposium (Intern.) on High Dynamic Pressures (C.E.A. Paris, France, 1978) pp. 3-8.
[10] C.-S. Yoo and H. Cynn, J. Chem. Phys. **111**, 10229 (1999).
[11] Zaug, J.M., "Elastic Constants of β-HMX and Tantalum, Equation of State of Supercritical Fluids and Fluid Mixtures and Thermal Transport Determinations", in *Proc. Eleventh Detonation Symposium*, 1998, p. 498.
[12] Fickett and Davis, Detonations (University of California, Berkeley, 1979).
[13] J.-P. Poirier, Introduction to the Physics of the Earth's Interior (Cambridge University Press, Cambridge, UK, 1999), p. 64.
[14] R. Menikoff and T.D. Sewell, High Press. Res. **21**, 121 (2001).
[15] Dzyabchenko, A.V., Pivina, T.S., and Arnautova, E.A., J. Mol. Struct. **378**, 67 (1996).
[16] T.D. Sewell, J. Appl. Phys. **83**, 4142 (1998).
[17] D.C. Sorescu, B.M. Rice, and D.L. Thompson, J. Phys. Chem. B **102**, 6692 (1998).
[18] D.C. Sorescu, B.M. Rice, and D.L. Thompson, J. Phys. Chem. B **103**, 6783 (1999).
[19] J.P. Lewis, T.D. Sewell, R.B. Evans, and G.A. Voth, J. Phys. Chem. B **104**, 1009 (2000).
[20] Bedrov, D., Smith, G.D., and Sewell, T.D., *J. Chem. Phys.* **112**, 7203 (2000).
[21] Bedrov, D., Smith, G.D., and Sewell, T.D., *Chem. Phys. Letters* **324**, 64 (2000).
[22] Bedrov, D., Chakravarthy, A., Smith, G.D., Sewell, T.D., Menikoff, R., and Zaug, J.M., *J. Computer-Aided Materials Design* (in press, June 2002).
[23] Bedrov, D., Smith, G.D., Sewell, T.D., "Molecular Dynamics Simulations of HMX Crystal Polymorphs Using a Flexible Molecule Force Field," to appear in "Shock Compression of Condensed Matter – 2001", M.D. Furnish, Ed.
[24] Sewell, Bedrov, Smith, "Elastic Properties of HMX," to appear in: Shock Compression of Condensed Matter – 2001", M.D. Furnish, Ed..
[25] D.C. Sorescu, B.M. Rice, and D.L. Thompson, J. Phys. Chem. A **102**, 8386 (1998).
[26] Smith, G.D., and Bharadwaj, R.K., *J. Phys. Chem. B* **103**, 3570 (1999).
[27] Parrinello, M., and Rahman, A., *J. Chem. Phys.* **76**, 2662 (1982).
[28] Allen, M.P., and Tildesley, D.J., *Computer Simulation of Liquids* (Oxford University Press, Oxford, 1987).
[29] Landau, L.D.; Lifschitz, E.M. *Theory of Elasticity* (Pergammon Press, Oxford, 1970) Subsection 10.
[30] B. Olinger, P.M. Halleck, and H.H. Cady, J. Chem. Phys. **62**, 4480 (1975); and references therein.
[31] Tsai, S.W. Mechanics of Composite Materials, Part II, Theoretical Aspects, AFML Tech. Rept. AFML-TR-66-149, November, 1966.

[1] M.R. Baer, Thermochim. Acta **38**, 351 (2002).
[2] S.G. Bardenhagen, J.U. Brackbill, and D. Sulsky, Phys. Rev. E **62**, 3882 (2000).
[3] R. Menikoff and T.D. Sewell, Combust. Theor. Model. **6**, 103 (2002).
[4] Gibbs, T.R.; Popolato, A. *LASL Explosive Property Data* (University of California, Berkeley, 1980).
[5] C.S Choi and H.P. Boutin, Acta Crystallogr. B **26**, 1235 (1970).
[6] Kohno, Y.; Maekawa, K.; Azuma, N.; Tsuchioka, T.; Hashizume, T.; Imamura, A. *Kogyo Kayako* **53**, 227 (1992).
[7] Cady, H.H.; Larson, A.C.; Cromer, D.T. *Acta Cryst.* **16**, 617 **(1963)**. Note that the "*y*" fractional coordinate for atom N_1 in Table 2 should have a negative sign.
[8] Cobbledick, R.E.; Small, R. W. H. *Acta Cryst. B* **30**, 1918 (1974).
[9] B. Olinger, B. Roof, and H. Cady, "The linear and volume compression of β-HMX and RDX", in: Proc. Symposium (Intern.) on High Dynamic Pressures (C.E.A. Paris, France, 1978) pp. 3-8.
[10] C.-S. Yoo and H. Cynn, J. Chem. Phys. **111**, 10229 (1999).
[11] Zaug, J.M., "Elastic Constants of β-HMX and Tantalum, Equation of State of Supercritical Fluids and Fluid Mixtures and Thermal Transport Determinations", in *Proc. Eleventh Detonation Symposium*, 1998, p. 498.
[12] Fickett and Davis, Detonations (University of California, Berkeley, 1979).
[13] J.-P. Poirier, Introduction to the Physics of the Earth's Interior (Cambridge University Press, Cambridge, UK, 1999), p. 64.
[14] R. Menikoff and T.D. Sewell, High Press. Res. **21**, 121 (2001).
[15] Dzyabchenko, A.V., Pivina, T.S., and Arnautova, E.A., J. Mol. Struct. **378**, 67 (1996).
[16] T.D. Sewell, J. Appl. Phys. **83**, 4142 (1998).
[17] D.C. Sorescu, B.M. Rice, and D.L. Thompson, J. Phys. Chem. B **102**, 6692 (1998).
[18] D.C. Sorescu, B.M. Rice, and D.L. Thompson, J. Phys. Chem. B **103**, 6783 (1999).
[19] J.P. Lewis, T.D. Sewell, R.B. Evans, and G.A. Voth, J. Phys. Chem. B **104**, 1009 (2000).
[20] Bedrov, D., Smith, G.D., and Sewell, T.D., *J. Chem. Phys.* **112**, 7203 (2000).
[21] Bedrov, D., Smith, G.D., and Sewell, T.D., *Chem. Phys. Letters* **324**, 64 (2000).
[22] Bedrov, D., Chakravarthy, A., Smith, G.D., Sewell, T.D., Menikoff, R., and Zaug, J.M., *J. Computer-Aided Materials Design* (in press, June 2002).
[23] Bedrov, D., Smith, G.D., Sewell, T.D., "Molecular Dynamics Simulations of HMX Crystal Polymorphs Using a Flexible Molecule Force Field," to appear in "Shock Compression of Condensed Matter – 2001", proceedings of the 2001 American Physical Society Topical Conference on Shock Compression in Condensed Matter, 24-29 June 2001, Atlanta, GA; M.D. Furnish, Ed.
[24] Sewell, Bedrov, Smith, "Elastic Properties of HMX," to appear in: Shock Compression of Condensed Matter – 2001", proceedings of the 2001 American Physical Society Topical Conference on Shock Compression of Condensed Matter, 24-29 June 2001, Atlanta, GA; M.D. Furnish, Ed..
[25] D.C. Sorescu, B.M. Rice, and D.L. Thompson, J. Phys. Chem. A **102**, 8386 (1998).
[26] Smith, G.D., and Bharadwaj, R.K., *J. Phys. Chem. B* **103**, 3570 (1999).
[27] Parrinello, M., and Rahman, A., *J. Chem. Phys.* **76**, 2662 (1982).

[28] Allen, M.P., and Tildesley, D.J., *Computer Simulation of Liquids* (Oxford University Press, Oxford, 1987).
[29] Landau, L.D.; Lifschitz, E.M. *Theory of Elasticity* (Pergammon Press, Oxford, 1970) Subsection 10.
[30] B. Olinger, P.M. Halleck, and H.H. Cady, J. Chem. Phys. **62**, 4480 (1975); and references therein.
[31] Tsai, S.W. Mechanics of Composite Materials, Part II, Theoretical Aspects, AFML Tech. Rept. AFML-TR-66-149, November 1966.